ACS OMEGA

http://pubs.acs.org/journal/acsodf

Article

Cr(VI)-Mediated Homogeneous Fenton Oxidation for Decolorization of Methylene Blue Dye: Sludge Free and Pertinent to a Wide pH Range

Varuna S. Watwe, Sunil D. Kulkarni, and Preeti S. Kulkarni*

Cite This: *ACS Omega* 2021, 6, 27288−27296

Read Online

ACCESS | Metrics & More | Article Recommendations | Supporting Information

ABSTRACT: Fe(II)-mediated Fenton process is commonly employed for oxidative degradation of recalcitrant pollutants in wastewater. However, the method suffers from limitations like narrow working pH range and iron sludge formation. The present work deals with the degradation of Methylene Blue (MB) dye using Fenton-like oxidation by replacing Fe(II) with Cr(VI), which eliminates the limitations of classical Fenton oxidation. The Fenton-like oxidation of MB is brought about by HO• radicals generated by the disproportionation of chromium-coordinated peroxo complexes. It was observed that the working pH range for the Cr(VI)-mediated Fenton oxidation was 3−10, and no sludge formation takes place up to four cycles as the oxidation remains in the pure solution phase. The complete mineralization of dye was confirmed by observing the decay of MB peaks by a spectrophotometer and cyclic voltammetry. The reaction parameters like pH of the solution, temperature, degradation time, concentrations of H_2O_2, Cr(VI), and MB were studied for optimal performance of the Cr(VI) as the catalyst. Kinetic studies revealed that the Cr(VI)-mediated Fenton reaction follows pseudo-first-order reaction kinetics and depends on the concentration of HO• radicals. The proposed Cr(VI)-mediated Fenton oxidation in the present work is best suited for the degradation of organic dyes by adding H_2O_2 as a precursor in chromate-contaminated wastewaters.

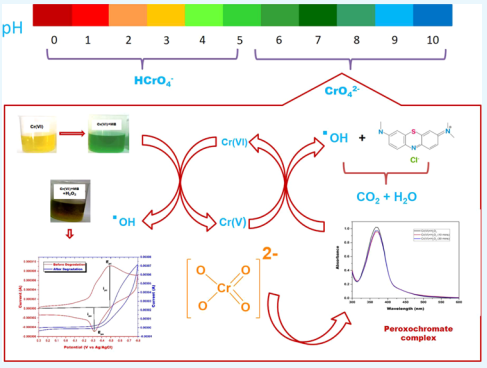

1. INTRODUCTION

The classical Fenton's process developed by Henry John Horstman Fenton in the 1890s is a widely used advanced oxidation process (AOP) to degrade organic contaminants. It involves the reaction between a solution of H_2O_2 and ferrous ions as a catalyst to oxidize recalcitrant pollutants in water.[1] The following two reactions are involved in the classical Fenton process.

$$Fe^{2+} + H_2O_2 \rightarrow Fe^{3+} + HO^{\bullet} + OH^{-} \quad (1)$$

$$Fe^{3+} + H_2O_2 \rightarrow Fe^{2+} + HOO^{\bullet} + H^{+} \quad (2)$$

$$HO^{\bullet} + \text{pollutant} \rightarrow CO_2 + H_2O \quad (3)$$

H_2O_2 oxidizes Fe(II) to give Fe(III), hydroxyl radical, and a hydroxyl ion in the first reaction. The Fe(III) is reduced to Fe(II) by another molecule of H_2O_2, giving a hydroperoxyl radical with a proton. The hydroxyl radical generated during this process is used in the nonselective degradation of recalcitrant organic pollutants, leading to the formation of CO_2 and H_2O. The HO• radical generated by degradation of hydrogen peroxide (H_2O_2) is a stronger oxidant with the standard potential of 2.8 V compared to pristine H_2O_2 having the standard potential of 1.78 V.[2] The generation of the HO• radical using H_2O_2 as a precursor has received a lot of attention from researchers because it is environmentally benign. Though the classical homogeneous Fenton process is facile, it lacks practical applications due to limitations like narrow pH range, secondary iron sludge generation, and Fe^{+2}/Fe^{+3} recycling. To overcome the limitations of the classical Fenton process, efforts have been made by many researchers to develop catalytic iron species composed of metal oxides,[3] metal salts,[4] zero-valent metal,[5] and nanocomposites.[6] These modifications avoid Fe(III) precipitation to some extent but lower the efficiency of oxidative degradation of organic pollutants by the HO• radical. They also lead to the unnecessary addition of total organic content to the wastewater.[7] Homogeneous and heterogeneous iron-based catalysts face practical difficulties in application. Thus, it is imperative to have an economically viable and practically applicable nonferrous Fenton catalyst, which will generate the HO• radical over a wide range of pH without generating any sludge or secondary organic compounds.[8] Metals like aluminum,[9] copper,[10] manganese,[11]

Received: July 31, 2021
Accepted: September 22, 2021
Published: October 5, 2021

ACS Publications

© 2021 The Authors. Published by American Chemical Society

cerium,[12] ruthenium,[13] and chromium[14] have been reported in the literature as nonferrous Fenton catalysts for the degradation of recalcitrant pollutants.

Among all of the above-mentioned nonferrous Fenton catalysts, chromium exhibits wide oxidation states ranging from −2 to +6. Out of the various oxidation states of chromium, Cr(III) and Cr(VI) species are commonly found in water bodies. Chromium being an oxyanion is soluble over the entire pH range.[15] The $HO^{\bullet}$ radical generation from the decomposition of H_2O_2 is mediated by the reduction of Cr(VI) to Cr(V) and Cr(IV). Even though chromium is economically and practically more viable than the iron-based Fenton catalyst, very few literature reports are available on the homogeneous chromium-based Fenton reaction to degrade recalcitrant pollutants. Degradation of 4-chlorophenol using a homogeneous chromium-based Fenton catalyst was first reported by Bokare et al.[14] To the best of our knowledge, no literature reports have yet been reported on the degradation of Methylene Blue (MB) dye using the homogeneous chromium-based Fenton reaction.

In the present work, $HO^{\bullet}$ radicals have been generated in situ from the reaction of Cr(VI) with H_2O_2 and used to degrade Methylene Blue (MB) dye. MB is a common cationic organic dye abundantly used in dying, feather, and textile industries. MB is a highly stable and water-soluble organic dye having antibiodegradable properties.[16] The effects of various experimental parameters like pH of the solution, concentration of Cr(VI), concentration of MB, concentration of H_2O_2, presence of different electrolytes, and reaction temperature have been studied. The kinetics of the degradation process is also studied. The reusability studies of the Cr(VI)/H_2O_2 system have also been carried out. Although Cr(VI) is one of the promising nonferrous Fenton catalysts, due to its high toxicity, its deliberate addition into wastewaters would not be sensible even though Cr(VI) can be removed post-treatment. The proposed process in the present work is more suited for chromate-contaminated wastewaters with recalcitrant pollutants. Every year, a large amount of Cr(VI)-containing wastewaters is generated from electroplating, metal finishing, leather tanning, and petroleum refining industries, requiring extensive treatment to prevent water contamination.[17] The addition of H_2O_2 to this Cr(VI)-contaminated industrial wastewater can be used to degrade organic dyes before its pretreatment. The present work can provide a cost-effective advanced oxidation technique for the degradation of Methylene Blue dye.

2. RESULTS AND DISCUSSION

2.1. Decolorization of MB in Different Systems. The Cr(VI)/H_2O_2 system's combined oxidative chemical efficiency in an aqueous solution was evaluated using MB dye as the model substrate. Decolorization of MB in different systems is represented in Figure 1. It can be seen from Figure 1 that Cr(VI) and H_2O_2 solely cannot degrade MB but can degrade it only when present in combination with each other. This fact points out the reaction between Cr(VI) and H_2O_2, which produces $HO^{\bullet}$ radicals responsible for the oxidative degradation of MB. The presence of $HO^{\bullet}$ radicals was confirmed by adding methanol as a quenching agent in the Cr(VI)+H_2O_2+MB system. From Figure 1, it can be seen that the degradation of MB was quenched after the addition of methanol in the Cr(VI)+H_2O_2+MB system, indicating that $HO^{\bullet}$ radicals are responsible for the oxidative degradation of

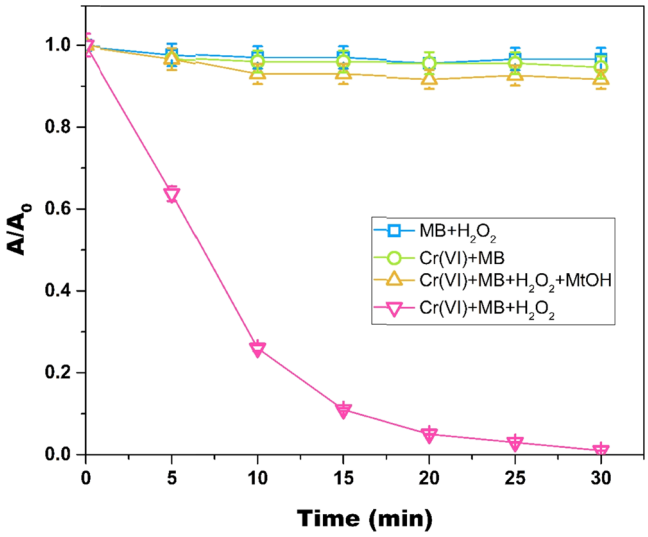

Figure 1. MB degradation in only Cr(VI), only H_2O_2, and Cr(VI)+H_2O_2 system at different time intervals (pH = 6; [H_2O_2] = 19.4 mM; [Cr(VI)] = 3 mM; [MB] = 15.7 μM; and temperature = 298 K). In the plot, A represents the absorbance at any given time "t" and A_0 represents the initial absorbance.

MB. The 99% decolorization of MB was observed in the optimum Cr(VI)/H_2O_2 system within 30 min.

The MB degradation in the Cr(VI)/H_2O_2 system was spectrophotometrically monitored in the present work. The decrease in absorbance of MB at 664 nm was regarded as a measure of its degradation. However, to confirm that the decrease in MB absorbance resulted from its complete mineralization and not just decolorization due to a redox reaction, further corroboration by another method was necessary. This confirmation was achieved by electrochemical studies. Cyclic voltammetric responses of the optimum Cr(VI)+MB system before and after the addition of H_2O_2 are shown in Figure 2. Cyclic voltammogram of Cr(VI)+MB before the addition of H_2O_2 showed a single cathodic signal at −0.5 V and a single anodic signal at −0.32 V. After the degradation of MB in the Cr(VI)/H_2O_2 system, anodic and cathodic peaks at −0.5 and −0.32 V disappeared, indicating the complete degradation of MB. Cyclic voltammograms of

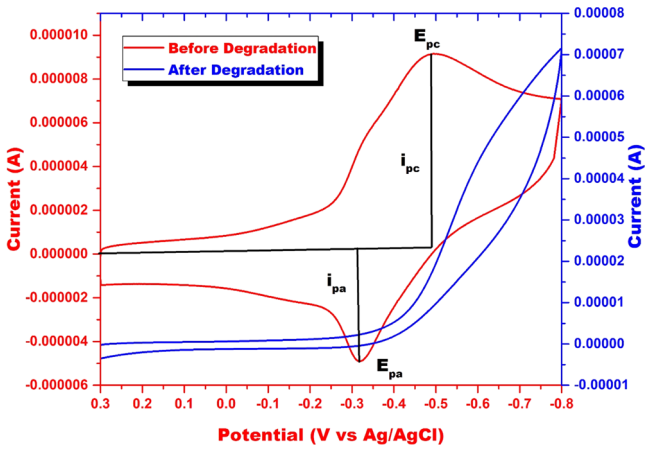

Figure 2. Cyclic voltammogram of MB in the Cr(VI)/H_2O_2 system before and after degradation (pH = 6; [H_2O_2] = 19.4 mM; [Cr(VI)] = 3 mM; [MB] = 15.7 μM; and temperature = 298 K).

https://doi.org/10.1021/acsomega.1c04090
ACS Omega 2021, 6, 27288−27296

Cr(VI)+MB in the presence and absence of H_2O_2 were recorded using KNO_3 as the supporting electrolyte and glassy carbon electrode as the working electrode in the potential range of 0.3 to −0.8 V versus Ag/AgCl as the reference electrode, with a scan rate of 0.1 V/s.[18,19] Only MB's anodic and cathodic signals are obtained using the conditions mentioned above, and Cr(VI) signals do not interfere with MB signals.

2.2. Effect of Initial pH. The pH of the solution plays a crucial role in all Fenton-like reactions. The solution's pH is directly related to the generation of $HO^{\bullet}$, which is responsible for the oxidative degradation of any substrate. To scrutinize the effect of pH on the mineralization of MB in the Cr(VI)-mediated Fenton oxidation, experiments were carried out at pH 2−10. Figure 3 illustrates the effect of pH on the

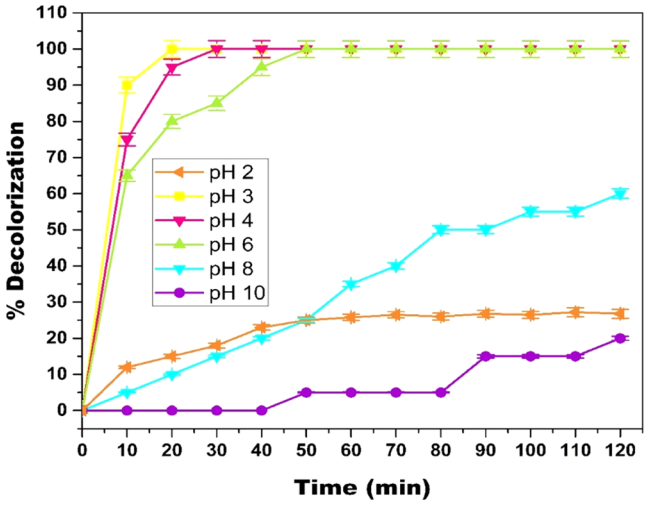

Figure 3. Effect of pH on MB degradation in the Cr(VI)/H_2O_2 system ([H_2O_2] = 19.4 mM; [Cr(VI)] = 3 mM; [MB] = 15.7 μM; and temperature = 298 K).

mineralization of MB. It can be observed from Figure 3 that as pH increases, the percentage decolorization of MB decreases. The maximum decolorization of MB was obtained at pH 3. The decolorization of MB is significantly inhibited at pH less than 3, which can be attributed to the high H^+ concentration, which acts as a $HO^{\bullet}$ radical scavenger[20] via eq 4. In addition, the H^+ ions of protonated H_2O_2 also act as a $HO^{\bullet}$ radical scavenger[21] via eq 5.

$$HO^{\bullet} + H^+ + e^- \rightarrow H_2O \quad (4)$$

$$H_2O_2 + H^+ \rightarrow H_3O_2^+ \quad (5)$$

The reason that acidic pH favors degradation is that at pH < 6, $HCrO_4^-$ is the predominant species and at pH ≥ 6, CrO_4^- species is dominant. $HCrO_4^-$ is a much stronger oxidant [E^0 ($HCrO_4^-/Cr^{+3}$ = 1.35 V_{SHE})] compared to CrO_4^- [E^0 ($CrO_4^-/Cr(OH)_3$ = −0.13 V_{SHE})]; hence, $HCrO_4^-$ promotes oxidation at a faster rate compared to CrO_4^-.[22] Thus, it can be concluded that acidic pH favors MB degradation. However, it is preferable to have a catalyst that can work at a circumneutral pH. Hence, pH 6, which gives almost 99% decolorization in 30 min, is considered as the optimal pH for MB decolorization for further optimizations.

2.3. Effects of Cr(VI) and H_2O_2 Concentration on the Decolorization of MB. To scrutinize the implementation of the Cr(VI)-mediated Fenton oxidation for decolorization of MB at pH 6, the effect of varying concentrations of Cr(VI) in the range of 1−7 mM and H_2O_2 in the range of 7.8−27.16 mM was evaluated, as illustrated in Figures 4 and 5 respectively. It

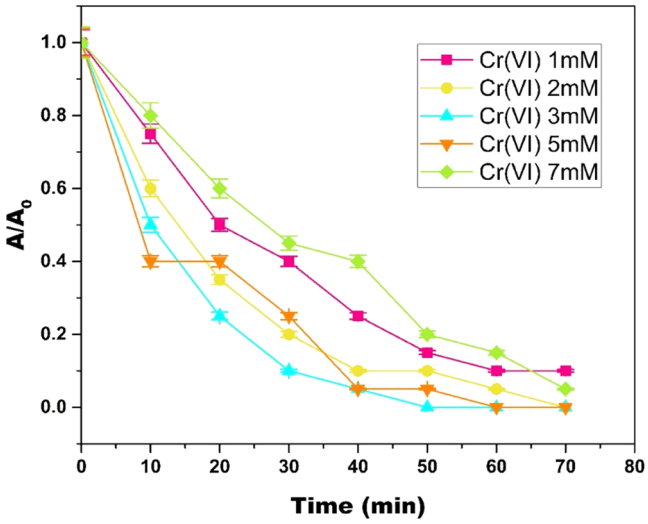

Figure 4. Effect of catalyst [Cr(VI)] concentration on MB degradation in the Cr(VI)/H_2O_2 system (pH = 6; [H_2O_2] = 19.4 mM; [MB] = 15.7 μM; and temperature = 298 K). In the plot, "A" represents the absorbance at any given time "t" and "A_0" represents the initial absorbance.

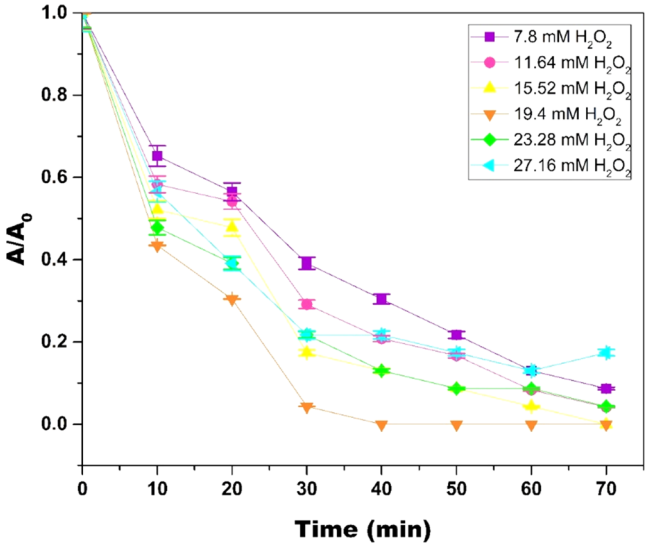

Figure 5. Effect of H_2O_2 concentration on MB degradation in the Cr(VI)/H_2O_2 system (pH = 6; [Cr(VI)] = 3 mM; [MB] = 15.7 μM; and temperature = 298 K). In the plot, "A" represents the absorbance at any given time "t" and "A_0" represents the initial absorbance.

was observed that with an initial increase in Cr(VI) and H_2O_2 concentration, the decolorization efficiency of MB increased until optimal concentration; 3 mM Cr(VI) and 19.4 mM H_2O_2 were reached. A further increase in the Cr(VI) and H_2O_2 concentrations resulted in a decrease in the decolorization of MB. The decrease in decolorization efficiency with an increase in reactant concentration can be attributed to excess reactants competing with MB to consume $HO^{\bullet}$ radicals; also, superfluous reactants slow down the formation of $HO^{\bullet}$ radicals.[23,24]

https://doi.org/10.1021/acsomega.1c04090
ACS Omega 2021, 6, 27288−27296

2.4. Optimum Ratio of Cr(VI)/H_2O_2 for Effective Decolorization. Since the MB dye degradation is initiated by the reaction between Cr(VI) and peroxide, along with the optimized concentrations of Cr(VI) and H_2O_2, the ratio of metal ions to H_2O_2 is also an essential parameter for a radical generation. Figure 6 illustrates the effect of change in the ratio

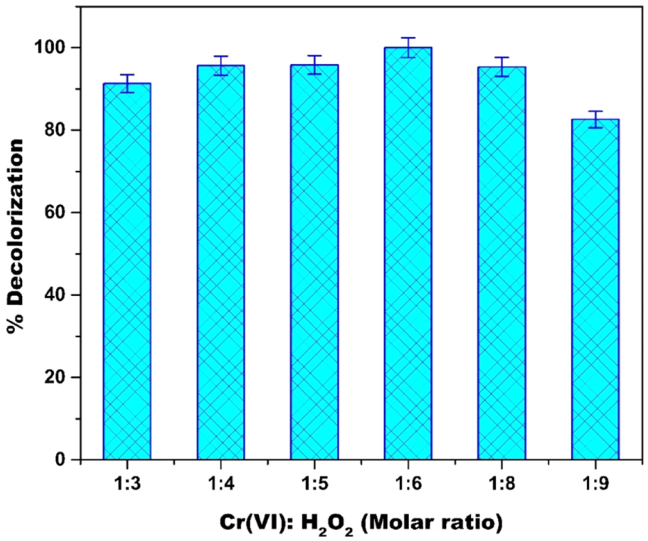

Figure 6. Effect of catalyst/oxidant ratio [Cr(VI)]/[H_2O_2] on MB degradation in the Cr(VI)/H_2O_2 system (pH = 6; [Cr(VI)] = 3 mM; [MB] = 15.7 μM; and temperature = 298 K).

of metal ion to H_2O_2 on the % decolorization of MB. From Figure 6, it can be seen that as the ratio of metal ion to H_2O_2 increases from 1:3 to 1:6, the percentage decolorization increases from 91.3 to 99, and as the ratio further increases from 1:6 to 1:9, the % decolorization decreases from 99 to 82.61. This decrease can be attributed to an excess reactant concentration that slows down the decolorization of MB by consuming HO$^\bullet$ radicals.[25]

2.5. Effect of Substrate Concentration on the Degree of Decolorization. The substrate's initial concentration is also an influential factor while studying its decolorization. To evaluate the effect of substrate concentration on the decolorization efficiency of the Cr(VI)-mediated Fenton oxidation, MB concentration was varied between 7.8 and 39.2 μM. Figure 7 shows the UV spectrum of fixed Cr(VI); 3 mM and different MB concentrations; 7.8−39.2 μM, before and after decolorization of MB. In Figure 7, for every concentration of MB, two peaks at 664 and 616 nm are observed, and no peak is observed after complete decolorization, indicating the complete degradation of MB in the Cr(VI)-mediated Fenton oxidation.

The percentage decolorization time is directly proportional to its initial MB concentration. As substrate concentration increases, more HO$^\bullet$ radicals are required for its decolorization, leading to a longer decolorization time. Table S1 shows different concentrations of MB and times required for its complete decolorization. The MB concentration was kept at 15.7 μM to obtain effective decolorization in a reasonable time.

2.6. Effect of Different Electrolytes on the Degree of Decolorization. Since wastewater samples contain many salts dissolved in them, the effect of dissolved salts on the chemical oxidation capacity of the Cr(VI)-mediated Fenton oxidation for MB degradation was investigated. The salt concentration

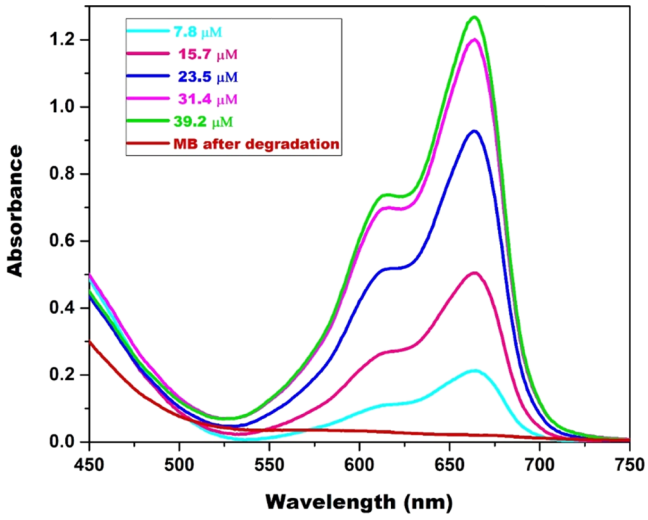

Figure 7. UV−visible spectrum of MB in the Cr(VI)/H_2O_2 system before and after degradation (pH = 6; [H_2O_2] = 19.4 mM; [Cr(VI)] = 3 mM; and temperature = 298 K).

was kept the same as that of the model substrate, MB (15.66 μM), and these experiments were carried out using optimal parameters. Table 1 illustrates the effect of dissolved

Table 1. Percentage MB Degradation in the Cr(VI)-Mediated Fenton Oxidation in the Presence of Different Electrolytes (pH = 6; [H_2O_2] = 19.4 mM; [Cr(VI)] = 3 mM; [MB] = 15.7 μM; Temperature = 298 K; and Electrolyte Concentration = 15.7 μM)

electrolyte	% degradation of MB
Na_2SO_4	98 ± 2.5
K_2SO_4	97 ± 2.5
NaCl	94 ± 2.1
KCl	92 ± 2.2
KBr	91 ± 2.1
KNO_3	98 ± 2.6
without electrolyte	99 ± 2.6

electrolytes on MB decolorization using the Cr(VI)-mediated Fenton oxidation. From Table 1, it can be seen that sulfate and nitrate salts do not interfere in the decolorization of MB. However, halide salts show a slight decrease in decolorization efficiency, and this decrease may be attributed to the presence of highly electronegative halide ions, which combine with HO$^\bullet$ radicals, inhibiting the decolorization of MB. Similar results have been obtained for MB decolorization by the classical Fenton reaction.[26]

2.7. Effect of Temperature on the Degree of Decolorization. Temperature plays a crucial role in the decomposition of H_2O_2, so the effect of an increase in temperature on decolorization efficiency of MB by the Cr(VI)-mediated Fenton oxidation was studied at 298, 308, and 318 K. From Figure 8, it can be revealed that the decolorization efficiency of MB decreases as the temperature increases from 298 to 318 K. At 298 K, 97% decolorization of MB is achieved in 30 min. In contrast, only 50% decolorization is obtained at 318 K. This decrease in percentage decolorization with an increase in temperature is due to the thermal decomposition of H_2O_2 in H_2O and O_2 at a higher temperature above 298 K.

https://doi.org/10.1021/acsomega.1c04090
ACS Omega 2021, 6, 27288−27296

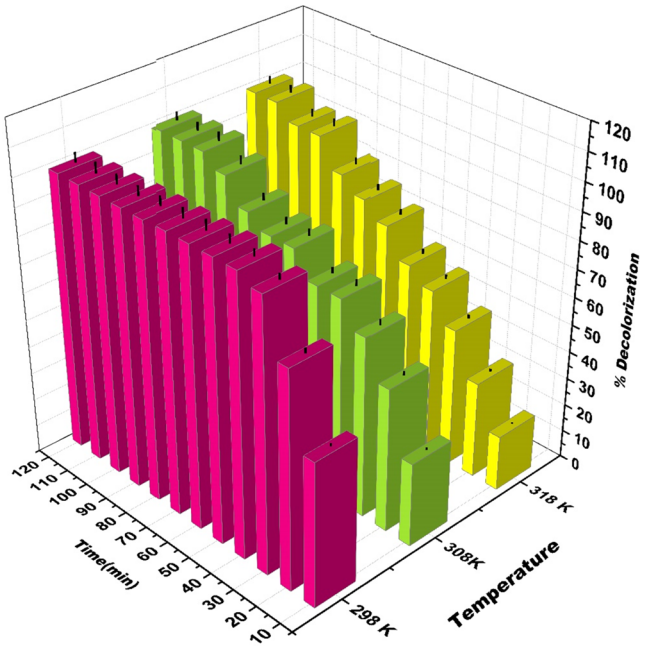

Figure 8. Effect of temperature on MB degradation in the Cr(VI)/H_2O_2 system (pH = 6; $[H_2O_2]$ = 19.4 mM; [Cr(VI)] = 3 mM; and [MB] = 15.7 μM).

Similar results are obtained in the literature for the classical Fenton reaction.[26,27]

2.8. Kinetics. The Cr(VI)-mediated Fenton oxidation reaction kinetics is complex and involves various reaction intermediates. The general rate law that represents the decolorization of MB is represented in eq 6[28]

$$\text{rate of MB decolorization} = -\frac{dC_{MB}}{dt} = k_{OH}C_{HO^{\bullet}}C_{MB} + \sum_{i}^{n} k_{Ox_i}C_{Ox_i}C_{MB} \quad (6)$$

where Ox_i represents radicals other than the HO$^{\bullet}$ radical, such as HOO$^{\bullet}$ radical; even though other radicals are present, the reaction rate depends only on the HO$^{\bullet}$ radical because it is present in higher concentrations and highly reactive than other radicals. Therefore

$$\text{rate of MB decolorization} = -\frac{dC_{MB}}{dt} = k_{OH}C_{HO^{\bullet}}C_{MB} \quad (7)$$

The concentration of reactive species quickly reaches a stationary state. Hence, the HO$^{\bullet}$ radical concentration is considered constant during fixed reaction conditions; hence, the rate of MB degradation is regarded as a pseudo-first-order, where the HO$^{\bullet}$ radical concentration is apparently constant.

$$\text{rate of MB decolorization} = -\frac{dC_{MB}}{dt} = k_1C_{MB} \quad (8)$$

where k_1 is the pseudo-first-order rate constant obtained by the product of k_{OH} and $C_{HO^{\bullet}}$, where the $C_{HO^{\bullet}}$ concentration is apparently constant.

$$\ln C_{MB} = \ln C_{MB_0} - k_1t \quad (9)$$

Equation 9 is obtained by integrating eq 8, as the concentration is directly proportional to absorbance by the Beer–Lambert law

$$\ln\left(\frac{A_{MB_t}}{A_{MB_0}}\right) = -k_1t \quad (10)$$

where A_{MB_t} is the absorbance of MB at any given time "t" and A_{MB_0} is the initial absorbance of MB in the reaction system before adding oxidant (H_2O_2).

Table 2 shows the values of the pseudo-first-order rate constant at different H_2O_2 and Cr(VI) concentrations with their respective R^2 values. From these values, it can be concluded that MB decolorization by Cr(VI)-mediated Fenton oxidation fits pseudo-first-order kinetics. It is also evident from k_1 values that as the Cr(VI) and H_2O_2 concentration increase above 3 and 19.4 mM, respectively, k_1 values decrease. Hence, 3 and 19.4 mM were chosen as optimal concentrations of Cr(VI) and H_2O_2, respectively.

Table 2. Pseudo-First-Order Kinetic Constants along with Regression Values at Different Cr(VI) and H_2O_2 Concentrations[a]

parameters		k_1 (min^{-1})	R^2
Cr(VI)	1 mM	0.039 ± 0.001	0.9893
	2 mM	0.049 ± 0.002	0.9808
	3 mM	0.076 ± 0.003	0.9974
	5 mM	0.062 ± 0.003	0.9066
	7 mM	0.032 ± 0.001	0.9652
H_2O_2	7.8 mM	0.032 ± 0.001	0.9848
	11.64 mM	0.039 ± 0.001	0.9771
	15.52 mM	0.051 ± 0.002	0.9779
	19.4 mM	0.098 ± 0.004	0.9011
	23.28 mM	0.042 ± 0.001	0.9636
	27.16 mM	0.032 ± 0.001	0.9390

[a]When the Cr(VI) and H_2O_2 concentrations were varied, respectively, other parameters were held constant: pH = 6, temperature = 298 K, [MB] = 15.7 μM, [Cr(VI)] = 3 mM, and $[H_2O_2]$ = 19.4 mM.

2.9. Mechanism of MB Decolorization in the Cr(VI)-Mediated Fenton Oxidation. Chromium exists as Cr(III) and Cr(VI) in the aqueous system. Both the oxidation states exist as oxyanions and are entirely soluble over the entire pH range[15] from 1 to 14. Cr(VI) plays a dual role of a catalyst and an oxidant in the reaction with H_2O_2 in the pH range 4.6–7.3. Cr(VI) exists as the oxyanions CrO_4^{2-}, $Cr_2O_7^{2-}$, $HCrO_4^{2-}$, and H_2CrO_4 depending on the solution's pH. The reaction between chromate ion and H_2O_2 is initiated by consecutive substitution of oxo ligands by peroxo groups. Figure 9 illustrates the schematic mechanism of the reaction between chromate and hydrogen peroxide to form HO$^{\bullet}$ radicals.[14,29,30] As illustrated in Figure 9, once peroxo groups substitute all oxo ligands, tetrakis(η^2-peroxo)chromate(V) anion complex is formed; this complex is metastable and further undergoes disproportionation reaction within the chromium coordination sphere producing chromate, singlet oxygen, and superoxide. These superoxides produced again react with tetra peroxochromate and generate HO$^{\bullet}$ radicals. These HO$^{\bullet}$ radicals further react with MB and degrade MB into intermediate products, followed by its conversion into CO_2 and H_2O.

https://doi.org/10.1021/acsomega.1c04090
ACS Omega 2021, 6, 27288–27296

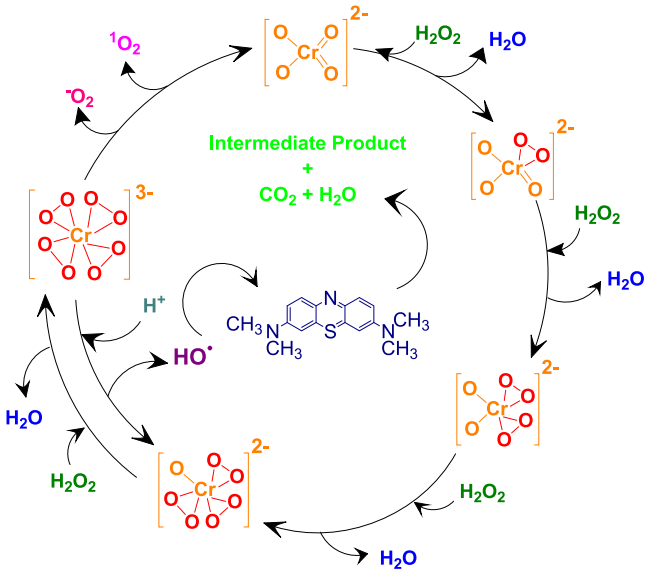

Figure 9. Schematic representation of complex chemistry between chromate and hydrogen peroxide.

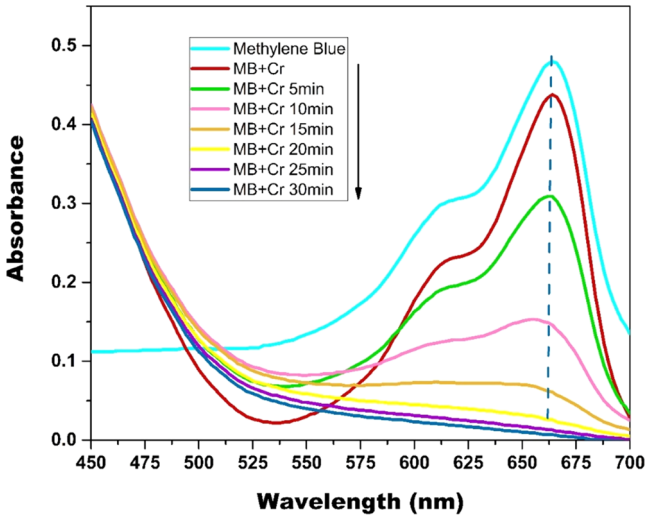

Figure 10. UV−visible spectra of MB at different time intervals in the Cr(VI)/H_2O_2 system. Reaction condition: [Cr(VI)] = 3 mM, [H_2O_2] = 19.4 mM, [MB]= 15.7 μM, temperature = 298 K; and pH = 6.

2.10. Identification of Primary Reactive Radical. The direct determination of HO$^\bullet$ radicals is difficult due to the short lifetime of HO$^\bullet$ radicals ($\sim 10^{-9}$ s). Hence, the formation of hydroxyl radicals was indirectly confirmed by a modified coumarin assay.[31] The linear increase in fluorescence intensity with respect to the experimental period indicates that hydroxyl radicals are generated, and their concentration increases with respect to time (Figure S1). It can be observed from Figure S1 that HO$^\bullet$ radicals are the primary active species in the Cr(VI)/H_2O_2 system.

2.11. Mineralization Studies. The fluorescence experiment indicates HO$^\bullet$ radicals to be present in the Cr(VI)/H_2O_2 system as primary reactive species. The HO$^\bullet$ radicals generated from the redox reaction between Cr(VI) and H_2O_2 are responsible for the mineralization of MB. To evaluate the percentage mineralization of MB in the Cr(VI)/H_2O_2 system, a total organic carbon (TOC) analysis of Cr(VI)+H_2O_2+MB was carried out at different time intervals. The results revealed that 32.5% TOC removal of 15.7 μM MB in the Cr(VI)/H_2O_2 system was achieved at pH 6 after reacting for 15 min and then reached 45.6 and 61% after reacting for 30 and 60 min, respectively. The removal percentage of TOC increases with time due to further decomposition of formed intermediates.

To scrutinize the mechanism of MB degradation, the UV−visible spectrum of MB at different time intervals in the Cr(VI)/H_2O_2 system was recorded, as shown in Figure 10 The adsorption peak at 664 nm gradually decreases with an increase in treatment time, and the adsorption peak at 664 nm was slightly blue-shifted.

2.12. Reusability of the Cr(VI)-Mediated Fenton Oxidation. To evaluate the reusability of the Cr(VI) mediated Fenton oxidation, four cycles of MB degradation were studied (Figure 11). In reusability studies after the degradation of MB in the first cycle, a fresh aliquot of 25 mL of 15.7 μM MB was added to the same reaction mixture. It was observed that in the first cycle, 99% MB degradation was achieved in 30 min, in the second cycle, 62% decolorization was achieved in 30 min, and complete decolorization took 50 min. The same process was continued for two more cycles involving addition of fresh MB every time. In the third cycle, 58% decolorization of MB was achieved in 30 min, and complete decolorization took 130 min, whereas in the fourth cycle, 20% decolorization was achieved in 30 min and complete decolorization took 255 min. After the fourth cycle, the decolorization was less than 20% and took a longer time for complete decolorization (>8 h). Thus, reusability after the fourth cycle was found to be impractical. The total MB degradation achieved during four cycles using 3 mM Cr(VI) and 19.4 mM H_2O_2 is 62.8 μM.

Cr(VI) is highly toxic, and hence, is not advisable to be used as a catalyst; hence, in the present work, at the end of the fourth cycle, Cr(VI) was reduced to Cr(III) using H_2O_2 under highly acidic condition before it was disposed into the aqueous stream. The Cr(VI) concentration was monitored using the DPC method.

3. CONCLUSIONS

In the present work, the Cr(VI)-mediated Fenton oxidation was used for MB dye decolorization. The optimum parameters for effective MB decolorization were found to be 19.4 mM H_2O_2, 3 mM Cr(VI), 15.7 μM MB, Cr(VI)/H_2O_2 ratio 1:6, and temperature 298 K. The Cr(VI)-mediated Fenton oxidation was found to be effective for MB decolorization over a wide pH range of 3−8. The decolorization of MB was monitored using a UV spectrophotometer for all optimization experiments. Cyclic voltammetry was used along with a UV spectrophotometer to confirm that MB is mineralized in the Cr(VI)-mediated Fenton oxidation. The kinetic studies showed that the MB decolorization in the Cr(VI)-mediated Fenton oxidation follows pseudo-first-order kinetics. The reaction rate increases with an initial increase in Cr(VI) and H_2O_2 concentrations, but if Cr(VI) and H_2O_2 is present in excess amounts, the reaction rate decreases due to the scavenging of HO$^\bullet$ radicals. The homogeneous Cr(VI)-mediated Fenton oxidation was found stable and reusable up to four cycles with a total degradation of 62.8 μM MB. The advantage of homogeneous Cr(VI)-mediated Fenton oxidation over other heterogeneous Fenton catalysts is that no extra time and chemicals are required to recover the catalyst and its activation, and no secondary sludge generation occurs.

https://doi.org/10.1021/acsomega.1c04090
ACS Omega 2021, 6, 27288−27296

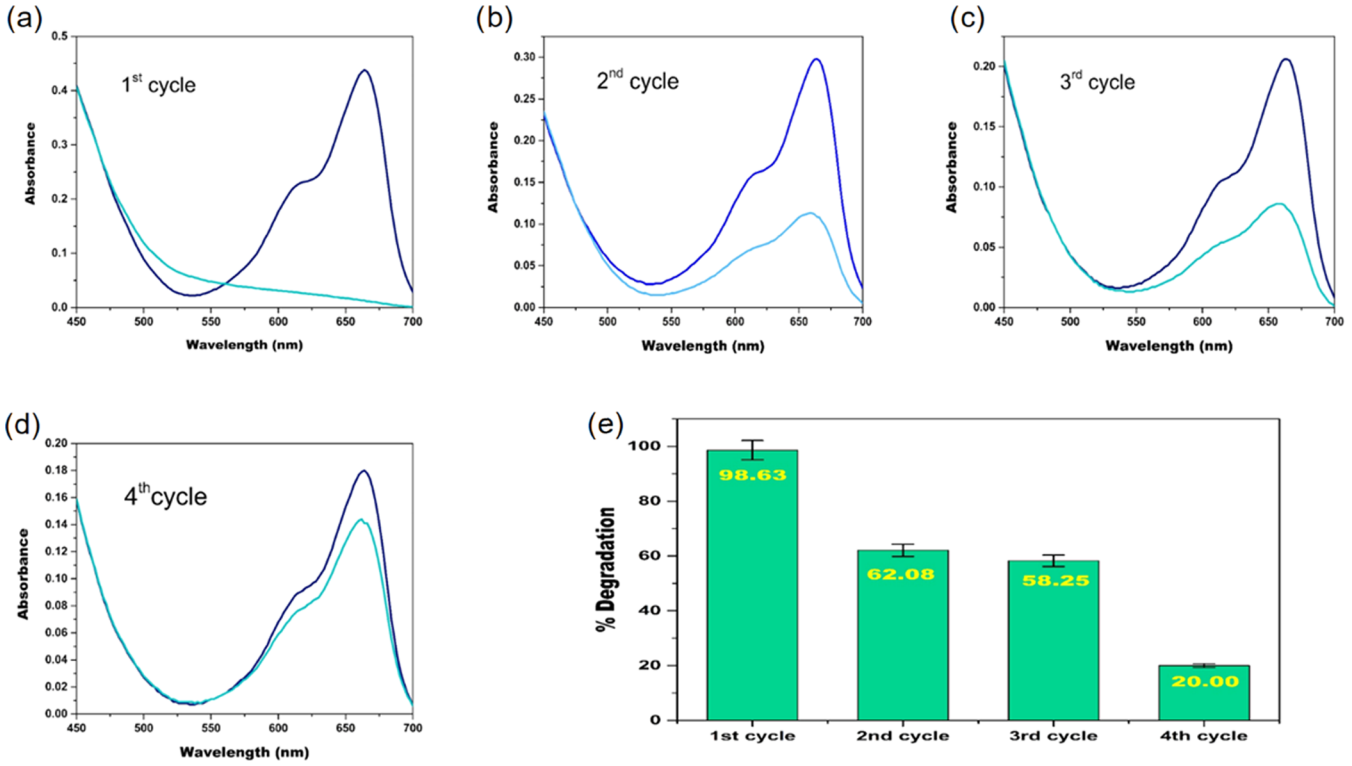

Figure 11. (a–d) UV spectrum of MB before and after degradation in first, second, third, and fourth cycles, respectively. (e) Bar graph of four degradation cycles along with percentage degradation of MB in each cycle (pH = 6; [H_2O_2] = 19.4 mM (total cycles); [Cr(VI)] = 3 mM (total cycles); [MB] = 15.7 μM (per cycle); and temperature = 298 K).

4. EXPERIMENTAL SECTION

4.1. Materials and Chemicals. All of the chemicals used in the present work were of analytical grade and used as received without any further purification. Potassium dichromate (99% pure) ($K_2Cr_2O_7$), sodium hydroxide (NaOH), Methylene Blue (MB), hydrogen peroxide (30% H_2O_2), sodium sulfate (Na_2SO_4), potassium sulfate (K_2SO_4), potassium nitrate (KNO_3), sodium chloride (NaCl), potassium chloride (KCl), potassium bromide (KBr), silver sulfate (Ag_2SO_4), mercuric sulfate ($HgSO_4$), ferrous ammonium sulfate (FAS), 1,10-phenanthroline, and 1,5-diphenyl carbazide (DPC) were obtained from Loba Chemie. Hydrochloric acid (HCl), sulfuric acid (H_2SO_4), and acetone were obtained from Qualigens. All of the solutions were prepared in deionized water obtained from Milli-Q ultrapure water.

4.2. Oxidation Reaction. All optimization experiments were carried out in 100 mL glass beakers under normal temperature–pressure conditions unless otherwise mentioned. Stock solutions of 100 mM Cr (VI) and 3 mM MB were prepared by dissolving 29.41 and 1 g of $K_2Cr_2O_7$ and MB, respectively, in 1 L of deionized water. Further aliquots from these stock solutions were taken out to prepare the required MB and Cr(VI) concentrations. pH experiments were carried out in a 100 mL glass beaker by adding 25 mL of 3 mM Cr(VI) and 25 mL of 15.7 μM MB sequentially. Five replicate beakers with the reaction mixture were prepared. The solution's pH in the beakers was adjusted to 2, 3, 4, 6, 8, and 10, respectively, using 0.1 M NaOH or 0.1 M HCl. After pH adjustment, 100 μL of 30% H_2O_2 (19.4 mM) was added to each beaker, and the time was recorded. The reaction mixture (5 mL) was taken out at intervals of 10 min after the addition of H_2O_2, and its absorbance was recorded at λ = 665 nm using a UV–visible spectrophotometer. After recording absorbance, the aliquot taken out was again added to the reaction mixture. The optimum amount of H_2O_2 required for the effective decolorization of MB was determined by varying it in the range of 7.8–27.2 mM, respectively, in solutions containing 25 mL of 3 mM Cr(VI) and 25 mL of 15.7 μM MB. The Cr(VI) concentration was optimized by keeping the amounts of MB (25 mL 15.7 μM) and H_2O_2 (19.4 mM) fixed in the reaction mixture and varying the Cr(VI) concentration (1, 2, 3, 5, and 7 mM respectively). The amount of MB for effective decolorization was optimized by keeping Cr(VI) (25 mL 3 mM) fixed in five different beakers. The concentrations of MB added to the five beakers were 7.8, 15.7, 23.5, 31.4, and 39.2 μM, respectively. The concentration of H_2O_2 added to each beaker was kept fixed at 19.4 mM. The presence of electrolytes in wastewater is inevitable. The effect of dissolved electrolytes on MB degradation was studied by adding 15.7 μM KCl/Na_2SO_4/K_2SO_4/KBr/KNO_3 to the optimal reaction mixture of Cr(VI), MB, and H_2O_2. The MB decolorization by Cr(VI)-mediated Fenton oxidation was studied by carrying out the reaction at three different temperatures, namely, 298, 308, and 318 K. The reaction mixture was kept identical in all three cases. The temperature of the reaction mixture was maintained using a thermostat.

4.3. Analysis. The monitoring of MB decolorization in the Cr (VI)-mediated Fenton oxidation was done by taking out an aliquot from the reaction mixture at intervals of 10 min till complete decolorization of MB was achieved. The absorbance value of the MB aliquot taken out was measured using a UV–visible spectrophotometer at λ = 665 nm. The degradation efficiency of MB was calculated using eq 11

https://doi.org/10.1021/acsomega.1c04090
ACS Omega 2021, 6, 27288–27296

$$\%\ \text{degradation efficiency} = \frac{MB_0 - MB_t}{MB_0} \times 100 \quad (11)$$

where MB_0 corresponds to the absorbance of MB before the addition of H_2O_2 and MB_t corresponds to the absorbance of MB after the addition of H_2O_2 at any time interval "t" during the reaction.

Cr(VI) concentration in Cr(VI)-mediated Fenton oxidation was measured by taking a fixed aliquot of sample from the system periodically and reacting it with 1,5-diphenyl carbazide reagent.[32] The absorbance of the Cr(VI)-DPC complex was measured spectrophotometrically at λ = 540 nm. The change in Cr(VI) concentration was calculated using eq 12

$$\text{Cr(VI) concentration} = \frac{C_0 - C_t}{C_0} \quad (12)$$

where C_0 corresponds to the initial Cr(VI) concentration and C_t corresponds to the Cr(VI) concentration at any time "t."

Along with a UV spectrophotometer, decolorization of MB was corroborated electrochemically using a potentiostat. MB in the reaction mixture was confirmed electrochemically using a 600E potentiostat (CH Instruments). The glassy carbon (GC) (CH Instruments) was used as the working electrode, platinum wire served as the counter electrode, and Ag/AgCl (CH Instrument) was used as the reference electrode. GC electrode surface was polished with alumina after every scan. All electrochemical experiments were carried out in a glass cell of capacity 20 cm^3 sealed with a Teflon cap at room temperature. For MB electrochemical measurements, a fixed aliquot was taken out from the Cr(VI)/H_2O_2+MB system and a fixed amount of KNO_3 as the supporting electrolyte was added. The total organic carbon (TOC) analysis was done using a TOC analyzer (Analyzer TOC Evolution VUV, Seres OL). For each TOC analysis, 50 mL of MB solution was analyzed and the scavenging agent (0.1 M Na_2SO_3) was immediately added to the MB sample to quench residual H_2O_2 so that accurate TOC values were obtained. The $HO^\bullet$ radicals were analyzed using a modified coumarin assay.

■ ASSOCIATED CONTENT

Supporting Information

The Supporting Information is available free of charge at https://pubs.acs.org/doi/10.1021/acsomega.1c04090.

Time required for complete MB decolorization at different MB concentrations (Table S1) and a fluorescence plot of 7-hydroxycoumarin (Figure S1) (PDF)

■ AUTHOR INFORMATION

Corresponding Author

Preeti S. Kulkarni − *Post-graduate and Research Centre, Department of Chemistry, MES Abasaheb Garware College, Pune 411004, India;* orcid.org/0000-0002-8604-878X; Phone: +9120 41038200; Email: psk.agc@mespune.in

Authors

Varuna S. Watwe − *Post-graduate and Research Centre, Department of Chemistry, MES Abasaheb Garware College, Pune 411004, India*

Sunil D. Kulkarni − *Post-graduate and Research Centre, Department of Chemistry, S. P. Mandali's Sir Parashurambhau College, Pune 411030, India;* orcid.org/0000-0001-6555-837X

Complete contact information is available at: https://pubs.acs.org/10.1021/acsomega.1c04090

Notes

The authors declare no competing financial interest.

■ ACKNOWLEDGMENTS

The authors are thankful to Principal, Maharashtra Education Society's Abasaheb Garware College Prof. P. B. Buchade for providing the infrastructure and cyclic voltammetry facility in DST FIST Laboratory for the present work. They also thank Dr. Anup N. Kate for his help during cyclic voltammetry experiments.

■ REFERENCES

(1) Fenton, H. J. H. LXXIII. - Oxidation of Tartaric Acid in Presence of Iron. *J. Chem. Soc. Trans.* **1894**, *65*, 899−910.

(2) Wang, Q.; Tian, S.; Ning, P. Degradation Mechanism of Methylene Blue in a Heterogeneous Fenton-like Reaction Catalyzed by Ferrocene. *Ind. Eng. Chem. Res.* **2014**, *53*, 643−649.

(3) Espinosa, J. C.; Catalá, C.; Navalón, S.; Ferrer, B.; Álvaro, M.; García, H. Iron Oxide Nanoparticles Supported on Diamond Nanoparticles as Efficient and Stable Catalyst for the Visible Light Assisted Fenton Reaction. *Appl. Catal., B* **2018**, *226*, 242−251.

(4) Huang, X.; Zhou, H.; Yue, X.; Ran, S.; Zhu, J. Novel Magnetic Fe3O4/α-FeOOH Nanocomposites and Their Enhanced Mechanism for Tetracycline Hydrochloride Removal in the Visible Photo-Fenton Process. *ACS Omega* **2021**, *6*, 9095−9103.

(5) Ambika, S.; Devasena, M.; Nambi, I. M. Synthesis, Characterization and Performance of High Energy Ball Milled Meso-Scale Zero Valent Iron in Fenton Reaction. *J. Environ. Manage.* **2016**, *181*, 847−855.

(6) Bel Hadjltaief, H.; Da Costa, P.; Beaunier, P.; Gálvez, M. E.; Ben Zina, M. Fe-Clay-Plate as a Heterogeneous Catalyst in Photo-Fenton Oxidation of Phenol as Probe Molecule for Water Treatment. *Appl. Clay Sci.* **2014**, *91*−*92*, 46−54.

(7) Lee, C.; Sedlak, D. L. A Novel Homogeneous Fenton-like System with Fe(III)−Phosphotungstate for Oxidation of Organic Compounds at Neutral PH Values. *J. Mol. Catal. A* **2009**, *311*, 1−6.

(8) Bokare, A. D.; Choi, W. Review of Iron-Free Fenton-like Systems for Activating H_2O_2 in Advanced Oxidation Processes. *J. Hazard. Mater.* **2014**, *275*, 121−135.

(9) Lien, H.; Wilkin, R. Reductive Activation of Dioxygen for Degradation of Methyl Tert-Butyl Ether by Bifunctional Aluminum. *Environ. Sci. Technol.* **2002**, *36*, 4436−4440.

(10) Chen, T.; Zhu, Z.; Zhang, H.; Shen, X.; Qiu, Y.; Yin, D. Enhanced Removal of Veterinary Antibiotic Florfenicol by a Cu-Based Fenton-like Catalyst with Wide PH Adaptability and High Efficiency. *ACS Omega* **2019**, *4*, 1982−1994.

(11) Ding, J.; Sun, Y.-G.; Ma, Y.-L. Highly Stable Mn-Doped Metal−Organic Framework Fenton-Like Catalyst for the Removal of Wastewater Organic Pollutants at All Light Levels. *ACS Omega* **2021**, *6*, 2949−2955.

(12) Wang, S.; Jia, Y.; Song, L.; Zhang, H. Decolorization and Mineralization of Rhodamine B in Aqueous Solution with a Triple System of Cerium(IV)/H2O2/Hydroxylamine. *ACS Omega* **2018**, *3*, 18456−18465.

(13) Hu, Z.; Leung, C.-F.; Tsang, Y.-K.; Du, H.; Liang, H.; Qiu, Y.; Lau, T.-C. A Recyclable Polymer-Supported Ruthenium Catalyst for the Oxidative Degradation of Bisphenol A in Water Using Hydrogen Peroxide. *New J. Chem.* **2011**, *35*, 149−155.

(14) Bokare, A. D.; Choi, W. Chromate-Induced Activation of Hydrogen Peroxide for Oxidative Degradation of Aqueous Organic Pollutants. *Environ. Sci. Technol.* **2010**, *44*, 7232−7237.

(15) Beverskog, B.; Puigdomenech, I. Revised Pourbaix Diagrams for Chromium at 25-300 °C. *Corros. Sci.* **1997**, *39*, 43−57.
(16) Kulkarni, P.; Watwe, V.; Doltade, T.; Kulkarni, S. Fractal Kinetics for Sorption of Methylene Blue Dye at the Interface of Alginate Fullers Earth Composite Beads. *J. Mol. Liq.* **2021**, *336*, No. 116225.
(17) Owlad, M.; Aroua, M. K.; Daud, W. A. W.; Baroutian, S. Removal of Hexavalent Chromium-Contaminated Water and Wastewater: A Review. *Water, Air, Soil Pollut.* **2009**, *200*, 59−77.
(18) Chakraborty, A.; Ahamed, S.; Pal, S.; Saha, S. K. Cyclic Voltammetric Investigations of Thiazine Dyes on Modified Electrodes. *ISRN Electrochem.* **2013**, *2013*, No. 959128.
(19) Watwe, V.; Kulkarni, P. Evaluation of Cr (VI) Adsorption on Glutaraldehyde Crosslinked Chitosan Beads Using Cyclic Voltammetry Employing Gold Electrode. *J. Anal. Sci. Technol.* **2021**, *12*, No. 37.
(20) Ahmadi, M.; Ghanbari, F. Combination of UVC-LEDs and Ultrasound for Peroxymonosulfate Activation to Degrade Synthetic Dye: Influence of Promotional and Inhibitory Agents and Application for Real Wastewater. *Environ. Sci. Pollut. Res.* **2018**, *25*, 6003−6014.
(21) Devi, L. G.; Rajashekhar, K. E.; Raju, K. S. A.; Kumar, S. G. Kinetic Modeling Based on the Non-Linear Regression Analysis for the Degradation of Alizarin Red S by Advanced Photo Fenton Process Using Zero Valent Metallic Iron as the Catalyst. *J. Mol. Catal. A* **2009**, *314*, 88−94.
(22) Kulkarni, P. S.; Deshmukh, P. G.; Jakhade, A. P.; Kulkarni, S. D.; Chikate, R. C. 1,5 Diphenyl Carbazide Immobilized Cross-Linked Chitosan Films: An Integrated Approach towards Enhanced Removal of Cr(VI). *J. Mol. Liq.* **2017**, *247*, 254−261.
(23) Bergendahl, J. A.; Thies, T. P. Fenton's Oxidation of MTBE with Zero-Valent Iron. *Water Res.* **2004**, *38*, 327−334.
(24) Giwa, A.-R. A.; Bello, I. A.; Olabintan, A. B.; Bello, O. S.; Saleh, T. A. Kinetic and Thermodynamic Studies of Fenton Oxidative Decolorization of Methylene Blue. *Heliyon* **2020**, *6*, No. e04454.
(25) Neamtu, M.; Yediler, A.; Siminiceanu, I.; Kettrup, A. Oxidation of Commercial Reactive Azo Dye Aqueous Solutions by the Photo-Fenton and Fenton-like Processes. *J. Photochem. Photobiol. A* **2003**, *161*, 87−93.
(26) Dutta, K.; Mukhopadhyay, S.; Bhattacharjee, S.; Chaudhuri, B. Chemical Oxidation of Methylene Blue Using a Fenton-like Reaction. *J. Hazard. Mater.* **2001**, *84*, 57−71.
(27) Ramirez, J. H.; Costa, C. A.; Madeira, L. M. Experimental Design to Optimize the Degradation of the Synthetic Dye Orange II Using Fenton's Reagent. *Catal. Today* **2005**, *107−108*, 68−76.
(28) Núñez, L.; García-Hortal, J. A.; Torrades, F. Study of Kinetic Parameters Related to the Decolourization and Mineralization of Reactive Dyes from Textile Dyeing Using Fenton and Photo-Fenton Processes. *Dyes Pigm.* **2007**, *75*, 647−652.
(29) Pettine, M.; Campanella, L.; Millero, F. J. Reduction of Hexavalent Chromium by H2O2 in Acidic Solutions. *Environ. Sci. Technol.* **2002**, *36*, 901−907.
(30) Zhang, L.; Lay, P. A. EPR Spectroscopic Studies on the Formation of Chromium(V) Peroxo Complexes in the Reaction of Chromium(VI) with Hydrogen Peroxide. *Inorg. Chem.* **1998**, *37*, 1729−1733.
(31) Louit, G.; Foley, S.; Cabillic, J.; Coffigny, H.; Taran, F.; Valleix, A.; Renault, J. P.; Pin, S. The Reaction of Coumarin with the OH Radical Revisited: Hydroxylation Product Analysis Determined by Fluorescence and Chromatography. *Radiat. Phys. Chem.* **2005**, *72*, 119−124.
(32) Kulkarni, P. S.; Watwe, V. S.; Hipparge, A. J.; Sayyad, S. I.; Sonawane, R. A.; Kulkarni, S. D. Valorization of Uncharred Dry Leaves of Ficus Benjamina towards Cr (VI) Removal from Water: Efficacy Influencing Factors and Mechanism. *Sci. Rep.* **2019**, *9*, No. 19385.

https://doi.org/10.1021/acsomega.1c04090
ACS Omega 2021, 6, 27288−27296